Glyceraldehyde-3-phosphate dehydrogenase promotes cancer growth and metastasis through upregulation of SNAIL expression

KAIYAN LIU[1*], ZHENJIE TANG[2*], AMIN HUANG[3*], PING CHEN[1*], PANPAN LIU[1], JING YANG[1], WENHUA LU[1], JIANWEI LIAO[1], YICHENG SUN[1], SHIJUN WEN[1], YUMIN HU[1] and PENG HUANG[1,4]

[1]Sun Yat-sen University Cancer Center, State Key Laboratory of Oncology in South China, Collaborative Innovation Center for Cancer Medicine, Guangzhou, Guangdong 510060; [2]Department of Thoracic and Cardiovascular Surgery, Second Xiangya Hospital of Central South University, Changsha, Hunan 410011; [3]Department of Medical Oncology, The Eastern Hospital of The First Affiliated Hospital, Sun Yat-sen University, Guangzhou, Guangdong 510700, P.R. China; [4]Department of Translational Molecular Pathology, The University of Texas MD Anderson Cancer Center, Houston, TX 77030, USA

Received September 21, 2016; Accepted November 8, 2016

DOI: 10.3892/ijo.2016.3774

Abstract. Glyceraldehyde-3-phosphate dehydrogenase (GAPDH) plays an important role in multiple cellular functions including metabolism and gene transcription. Our previous study showed that GAPDH expression was elevated in colon cancer and further upregulated in liver metastatic tissues, suggesting a possilbe role of GAPDH in promoting cancer metastasis. The present study was designed to investigate the underlying mechanism, using multiple experimental approaches including genetic silencing of GAPDH expression by short hairpin RNA (shRNA) and biochemcial/molecular analyses of the key events involved in glycolytic metabolism and epithelial-mesenchymal transition (EMT). We showed that silencing of GAPDH expression resulted in a significant reduction of glycolysis in colon cancer cell lines, accompanied by a decrease in cell proliferation and an apparent change in cell morphology associated with alterations in actin expression and phalloidine staining patterns. Furthermore, GAPDH suppression also caused a downregulation of gene expression involved in cancer stem-like cells and EMT. CHIP assay and co-immunoprecipitation revealed that GAPDH physically interacted with the transcriptional factor Sp1 and enhance the expression of SNAIL, a major regulator of EMT. Suppression of GAPDH expression resulted in a signficant decrease in SNAIL expression, leading to inhibition of EMT and attenuation of colon cancer cell migration *in vitro* and reduced metastasis *in vivo*. Overall, the present study suggests that GAPDH plays an important role in cancer metastasis by affecting EMT through regulation of Sp1-mediated SNAIL expression.

Correspondence to: Professor Yumin Hu or Professor Peng Huang, Sun Yat-sen University Cancer Center, State Key Laboratory of Oncology in South China, Collaborative Innovation Center for Cancer Medicine, 651 Dongfeng Road East, Guangzhou, Guangdong 510060, P.R. China
E-mail: huym@sysucc.org.cn
E-mail: huangpeng@sysucc.org.cn

*Contributed equally

Abbreviations: GAPDH, glyceraldehyde-3-phosphate dehydrogenase; EMT, epithelial-mesenchymal transition; shRNA, short hairpin RNA; OCR, oxygen consumption rate; ECAR, extracellular acidification rate; NC, negative control

Key words: GAPDH, epithelial-mesenchymal transition, colon cancer, metastasis, glycolysis, SNAIL

Introduction

Colon cancer is one of the most common malignacies and the fourth most frequent cause of cancer death (1-4). Metastasis is a major cause of death in colon cancer patients. Although the 5-year survival rate for colon cancer patients in early stages without metastasis is high, this rate drops significantly in patients diagnosed with regional lymph node metastases and further decreases to less than 10% in patients with distant metastases (5-7). Major efforts in the recent years to improve the therapy for metastatic colon cancer patients include the development of drugs that target antiangiogenesis and inhibit EGFR signaling with noticeable success (8-10). Despite such progress, major challenges still remain in clinical treatment of colon cancer with distant metastasis. Understanding of the biological properties of the metastastic cancer cells and the underlying mechanisms would provide an important basis for the development of more effective agents and therapeutic strategies.

Glyceraldehyde-3-phosphate dehydrogenase (GAPDH) is a key enzyme that catalyzes the redox reaction in the glycolytic pathway by converting glyceraldehyde-3-phosphate to 1,3-bisphosphoglycerate with a reduction of NAD^+ to NADH. Although GAPDH has long been considered as a house-keeping enzyme and thus, commonly used as an internal reference in western blotting and RT-PCR analyses (11,12), accumulating evidence suggest that GAPDH may also play non-enzymatic

roles with diverse functions and distinct subcellular distributions including cytoplasma, cell membranes and nucleus (13-16). Its upregulation seems related to cancer development, evident by its higher expression in Dunning R-3327 rat prostatic adenocarcinoma cells compared to normal rat ventral prostate tissue (17). Furthermore, our previous study showed that GAPDH expression was elevated in colon cancer tissue and further increased in metastasis liver tissue (18), which suggests that GAPDH may contribute to colon cancer metastasis. These results indicate an important role of GAPDH in tumor growth and metastasis, and therefore may be a potential candidate as a molecular target for cancer therapy. However, the mechanism by which GAPDH promotes cancer growth and metastasis remains unclear.

The purpose of the present study was to use both *in vitro* and *in vivo* experimental systems to evaluate the role of GAPDH in colon cancer metastasis and to investigate the underlying mechanism. Both molecular and biochemical approaches were employed to test the biological consequences of GAPDH silencing and the relevant regulatory events. Since epithelial-mesenchymal transition (EMT) is tightly associated with the key events during cancer cell detachment from primary tumor site and seems to endow cell mobility and invasiveness (19), we evaluated the potential link between GAPDH and EMT in this study. Our results showed that GAPDH could physically interact with the transcriptional factor Sp1 and promote the expression of SNAIL, leading to EMT and an increased cell mobility and cancer metastasis.

Materials and methods

Cell culture and transfection. Human colon cell lines HCT116 and LoVo cells were purchased from the ATCC (Manassas, VA, USA). HT29 cell line was obtained from Shanghai Cell Bank (Shanghai, China). The GAPDH-knockdown HCT116 and LoVo cells (designated as HCT116 sh-GAP and LoVo sh-GAP, respectively) were established by stable transfection with short hairpin RNA (shRNA) against GAPDH as described below. The control cells (designated as HCT116-NC and LoVo-NC) were transfected with scrambled shRNA. HCT116 sh-GAP and HCT116-NC cells were cultured in McCoy's 5A medium supplemented with 10% fetal bovine serum (FBS; Sigma-Aldrich, St. Louis, MO, USA). LoVo sh-GAP and LoVo-NC were cultured in F12K medium supplemented with 10% FBS (Sigma-Aldrich). Cells were incubated at 37˚C in a humidified atmosphere with 5% CO_2 and were routinely sub-cultured using 0.25% (w/v) trypsin-EDTA solution to detach cells from the culture surface.

The short hairpin RNA (shRNA) expression plasmids (PGLV-H1-GFP/Puro) and lentiviral vectors containing GAPDH-shRNA (5'-GTATGACAACAGCCTCAAG-3') or scrambled shRNA (5'-TTCTCCGAACGTGTCACG-3') were obtained from Shanghai GenePharma, Co., Ltd. (Shanghai, China). HCT116 and LoVo cells were infected with lentiviral particles using the protocol recommended by the manufacturer, and the transfected cells were selected using 2.5 μg/ml puromycin. Silencing to GAPDH expression was confirmed by qRT-PCR and western blot analysis.

Antibodies and reagents. The following antibodies were used for immunoblotting analyses using standard western blotting procedures: E-cadherin, vimentin, β-catenin, SNAIL, α-tubulin (all from Cell Signaling Technology, Beverly, CA, USA), GAPDH (Abcam, Cambridge, UK), NOTCH3 (Cell Signaling Technology). Anti-mouse and anti-rabbit secondary antibodies conjugated with HRP were purchased from Santa Cruz Biotechnology (Santa Cruz, CA, USA). Matrigel and Transwell chambers were purchased from BD Biosciences (San Jose, CA, USA). TRIzol reagent and puromycin were purchased from Invitrogen (Carlsbad, CA, USA).

Assays of cellular metabolism. Lactate and glucose concentrations in the cell culture medium were measured using a SBA-40D analyzer (Institute of Biology, Shandong Academy of Sciences (Jinan, China). Each experiment was repeated at least three times independently. Cellular oxygen consumption rate (OCR) and extracellular acidification rate (ECAR) were measured by XF24 analyzer (Seahorse Bioscience, Inc., North Billerica, MA, USA). Briefly, cells were seeded in McCoy'5A medium at 40,000 cells/well in XF24 cell plate 24 h before the assay. On the day of the assay, the medium was changed to DMEM (without serum, no glucose, no bicarbonate, supplemented with 2 mM glutamine), and incubated at 37˚C in an incubator without CO_2 for 1 h before measurement of OCR and ECAR. Glucose (10 mM), oligomycin (3 mM) and 2-DG (0.1 M) were prepared in the Dulbecco's modified Eagle's medium (DMEM) and loaded onto ports A, B and C, respectively. Metabolic analysis was performed using the glycolytic stress test protocol recommended by the manufacturer. Glycolytic rate was estimated from the ECAR after the injection of glucose. Maximum glycolytic capacity was calculated by the rate of increase in ECAR after the injection of oligomycin following glucose. The glycolytic reserve was estimated using the difference between maximum glycolytic capacity and glycolytic rate. Glycolytic responds was determined using the ratio of maximum glycolytic capacity to glycolysis rate. Each assay was repeated at least 3 times.

Assay of GAPDH enzyme activities. GAPDH enzyme activity was measured using an assay kit (AM1639) purchased from Thermo Fisher Scientific. Cells were plated in 96-well plate (5,000 cells/well), 200 μl KDalert lysis buffer was added to each well, and the samples were then incubated at 4˚C for 15 min. The cell lysate was homogenized by pipetting up and down 4-5 times, and 10 μl of each lysate was transfered to a clean 96-well dark plate. Next, 90 μl of KDalert Master Mix was added to each well. The increase in fluorescence (the excitation wavelength at 560 nm and the emission wavelength at 590 nm) was measured every minute for up to 8 min at room temperature, using a Fluoroskan spectrometer.

Cell proliferation and colony formation assays. Cell proliferation was assessed using MTT assay. After the cells in 96-well plates were incubated with the MTT reagent (3-(4,5-dimethylthiazol-2-yl)-2,5-diphenyltetrazolium bromide) at 37˚C for 3 h, the culture medium was removed, and then 200 μl dimethyl sulfoxide (DMSO) was added to dissolve the formazan. The OD values were recorded at 569 nm using a microplate reader (Bio-Rad Laboratories, Hercules, CA, USA). For colony formation assay, cells were seeded in a 6-well plate (500 cells/well) and were cultured in McCoy'5A medium (HCT116

Table I. The primers used for qRT-PCR in the present study.

Genes	Forward primer	Reverse primer
GAPDH	5'-AATGGGCAGCCGTTAGGAAA-3'	5'-GCCCAATACGACCAAATCAGAG-3'
Actin	5'-AACTCCATCATGAAGTGTGACG-3'	5'-GATCCACATCTGCTGGAAGG-3'
ABCG2	5'-AGGCAGATGCCTTCTTCGTT-3'	5'-TGAGATTGACCAACAGACCATCA-3'
ALDH1	5'-GGCCCTCAGATTGACAAGGA-3'	5'-AACACTGTGGGCTGGACAAA-3'
NOTCH1	5'-GACAGCCTCAACGGGTACAA-3'	5'-CACACGTAGCCACTGGTCAT-3'
NOTCH3	5'-GCCAAGCGGCTAAAGGTAGA-3'	5'-ATTAGCGGGGTGAAGCCATC-3'
NANOG	5'-CAATGGTGTGACGCAGGGAT-3'	5'-TGCACCAGGTCTGAGTGTTC-3'
SOX2	5'-GGGGAAAGTAGTTTGCTGCC-3'	5'-CGCCGCCGATGATTGTTATT-3'
BMI1	5'-CTGGTTGCCCATTGACAGCG-3'	5'-AAAAATCCCGGAAAGAGCAGCC-3'
SNAIL	5'-CGAGTGGTTCTTCTGCGCTA-3'	5'-CTGCTGGAAGGTAAACTCTGGA-3'
α-Tublin	5'-GTCTCGCGTTGTTCTCTGGG-3'	5'-GCACTCACGCATGTTTTCCC-3'

cells) or F12 K medium (LoVo cells) supplemented with 10% FBS for 14 days. The cells were washed twice with phosphate-buffered saline (PBS), fixed with methanol for 15 min, and the colonies were stained with crystal violet for 15 min at room temperature. After the samples were washed with water and air-dried, colonies of >50 cells were counted.

RNA isolation and qRT-PCR. Total RNA was extracted from cultured cells with TRIzol and RNA concentration was calculated by measuring the OD value at 260 nm. RNA (0.5-1 μg) was reverse-transcribed using an M-MLV Reverse Transcriptase kit according to the manufacturer's protocol. The resulting cDNA (20 ng) was mixed with SYBR-Green Master Mix, amplified by PCR with the respective primers, and analyzed using the Universal Probe Library Center software (Bio-Rad Laboratories). The PCR primers used in the present study are listed in Table I.

Western blot analysis and co-immunoprecipitation (IP). For preparation of cell extracts, cells were washed twice with cold PBS, and lysed in RIPA lysis buffer containing protease inhibitors and phosphatase inhibitors on ice for 20 min. Proteins (30 μg) were separated by electrophoresis using 10% SDS-PAGE. After electrophoresis, proteins were transferred to polyvinylidene fluoride membranes (Millipore, Billerica, MA, USA), and incubated with the following primary antibodies at the dilutions recommended by the manufacturers: E-cadherin (1:1,000), vimentin (1:1,000), β-catenin (1:1,000), SNAIL (1:1,000), GAPDH (1:10,000) or NOTCH3 (1:1,000). The samples were incubated overnight at 4˚C on a rocking-platform, and then incubated with horseradish peroxidase-conjugated secondary antibody (dilution, 1:10,000) for 1 h at room temperature. Protein bands were visualized using enhanced chemiluminescence reagent ECL (Nanjing KeyGen Biotech, Co., Ltd., Nanjing, China). α-Tubulin was also probed as a loading control. Co-immunoprecipitation assays were performed using the Pierce Co-immunoprecipitation kits (Thermo Fisher Scientific, Rockford, IL, USA). Cell lysates were solubilized using Nonidet P-40 at a final concentration of 0.5%. Soluble fractions (200-600 μg) from cell lysates were incubated overnight at 4˚C with antibody-immobilized beads. Beads were then centrifuged at 1000 x g for 1 min, and washed three times with PBS before elution. The eluted proteins were heated at 90˚C for 5 min and analyzed by western blotting.

Chromatin immunoprecipitation (ChIP). The kit was used for ChIP assays according to the protocol recommended by the manufacturer (Active Motif, Carlsbad, CA, USA). Cells ($5x10^6$) were cross-linked with 1% formaldehyde, and DNA was isolated and sheared to an approximate length of 200-1000 bp by sonication using an SLPe sonicator (Branson Ultrasonics Corp., Danbury, CT, USA). Sheared DNA was incubated with 1.5 μg anti-GAPDH antibody or control IgG overnight at 4˚C, followed by immunoprecipitation with 20 μl of protein A beads. Enriched DNA was extracted from the DNA/antibody/protein A/beads complexes by proteinase K digestion and purified using spin columns. Promoter sequence was analyzed by PCR. *SNAIL* minimal promoter primers were as follows: forward primer, ATTCGTGGGTGCTCAAGAGG (nucleotide positions -103 to -84); reverse primer, GCCCAGTCCTGGTG AATCTC (nucleotide positions +31 to +50).

Cell migration and invasion assays. For 'wound healing' assay, cells were seeded in a 6-well culture plate, grown to 80% confluence, and then the plate was scratched across the surface of the cell monolayer with a sterile pipette tip. The cell debris was removed by washing with fresh medium. At the indicated time points (24-48 h), the cells that migrated into the wounded area or protruded from the border of the scratched area were visualized and photographed under an inverted microscope.

Cell migration ability was further assessed using 6.5-mm Transwell chambers. Cell invasion was assessed using the Matrigel invasion chambers (24-well DI kit from BD Biosciences). The assays were performed according to the manufacturer's instructions. Briefly, $5.0x10^5$ cells were suspended in serum-free medium and seeded into the upper chamber. The lower chamber was filled with medium containing 10% FBS. After 24 h of incubation, the migrated/invaded cells that passed the filter were fixed with 4% paraformaldehyde, stained with crystal violet solution and counted

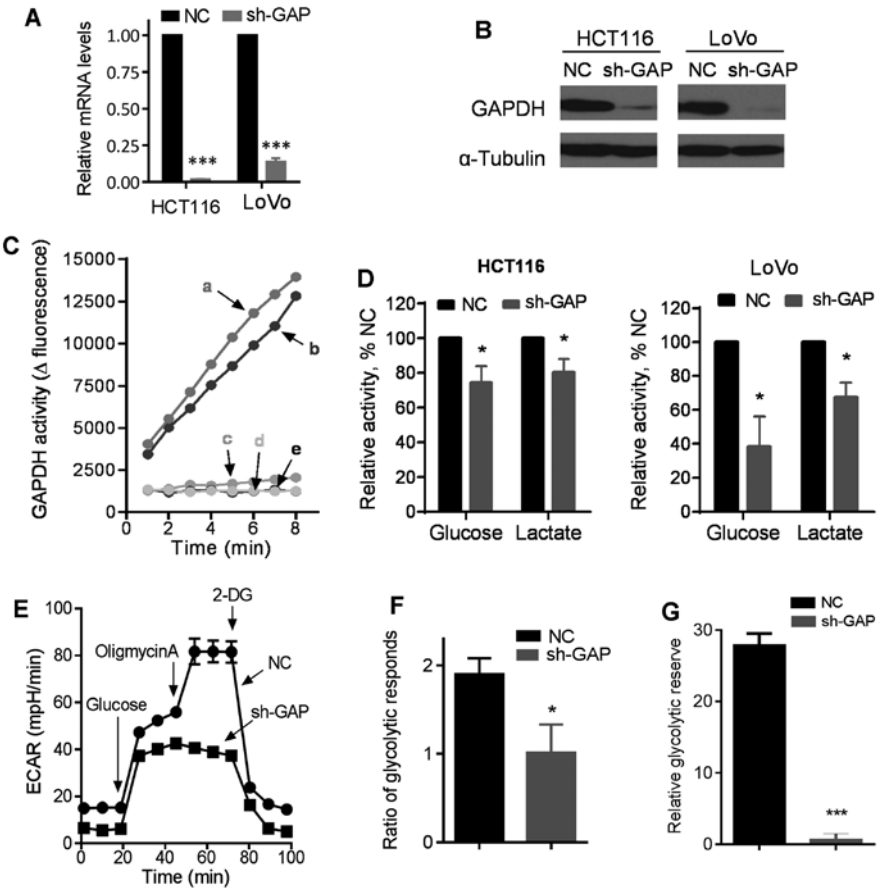

Figure 1. Impact of GAPDH silencing by shRNA on glucose metabolism in colon cancer cells. (A) Expression of GAPDH mRNA in HCT116 and LoVo cells infected with lentiviral vector containing shRNA (sh-GAP) or negative control shRNA (NC). (B) Western blot analysis of GAPDH levels in sh-GAP and NC cells. α-Tubulin was blotted as the protein loading control. (C) GAPDH enzyme activity was measured in sh-GAP and NC cell lines. a, b, c, d and e represent LoVo-NC, HCT116-NC, HCT116 sh-GAP, LoVo sh-GAP and black control, respectively. (D) Comparison of glucose consumption and lactate production in the medium of sh-GAP and NC cells in both HCT116 and LoVo cell pairs after cells were cultured in fresh medium for 12 h. (E) Glycolysis was measured by an XF24 metabolic analyzer using the glycolytic test kit provided by the manufacturer. A representative ECAR outputs in response to glucose, oligomycin, and 2-DG in HCT116 sh-GAP cells in comparison with HCT116-NC cells are shown. (F) Glycoytic respond ratios in HCT116 sh-GAP and HCT116NC were calculated from three separate experiments. (G) Relative glycoytic reserve calculated from three separate experiments. Data are shown as mean ± SD. n=3, *P<0.05, ***P<0.001.

under a microscope. The cell counts in five random fields were averaged for each filter from triplicate experiments.

Phalloidine staining of F-actin. Cells were fixed with absolute ethyl alcohol for 20 min and permeabilized with 0.25% of Triton X-100 in PBS at room temperature for 10 min. Samples were blocked with 1% of bovine serum albumin (BSA; Sigma-Aldrich) and incubated with fluorescent phalloidine for 30 min in the dark environment at room temperature, then washed with PBS for 3 times. The samples were also stained with DAPI for 3 min in the dark environment at room temperature and washed with PBS for 3 times to reveal the nuclei. Cells were observed under a scanning confocal microscope (Olympus FV10i; Olympus).

Xenograft model of tumor growth and metastasis. To evaluate the impact of GAPDH on tumor growth *in vivo*, 1.5x10^6 cells (NC control or sh-GAP) were subcutaneously innoculated into the left or right axilla of BALB/C nude mice (5 mice/group). Tumor length (L) and width (W) were measured twice a week using a caliper, and tumor volume was calculated using the formula: V = (W^2 x l)/2. After 3 weeks, the mice were sacrificed and the tumors were dissected for comparison. To analyze metastasis, 1.5x10^6 HCT116-NC or HCT116 sh-GAP cells were injected into BALB/C nude mice (12 mice/group) through tail vein. After one and a half months, mice were sacrificed and the lungs were isolated and inspected for metastasis. Both primary and metastatic tumors were isolated for imaging and pathological/histological analyses. The animal experiments were performed in complaince with the protocol and procedures approved by the Institutional Animal Care and Use Committee of Sun Yat-sen University Cancer Center.

Tumor specimens, H&E staining and immunohistochemistry. Tumor specimens embedded in paraffin slides were subjected to H&E staining and immunohistochemistry as previously described (18). For immunohistochemistry, paraffin embedded specimens were first treated with 3% H_2O_2 for 30 min to quench the endogenous peroxidase activity. The slides were then immersed in citrate buffer, heated for 5 min at 100˚C. After cooling, blocking with 10% goat serum. Rabbit monoclonal antibody against human GAPDH, biotinylated goat anti-rabbit antibody, and streptavidin-peroxidase conjugate

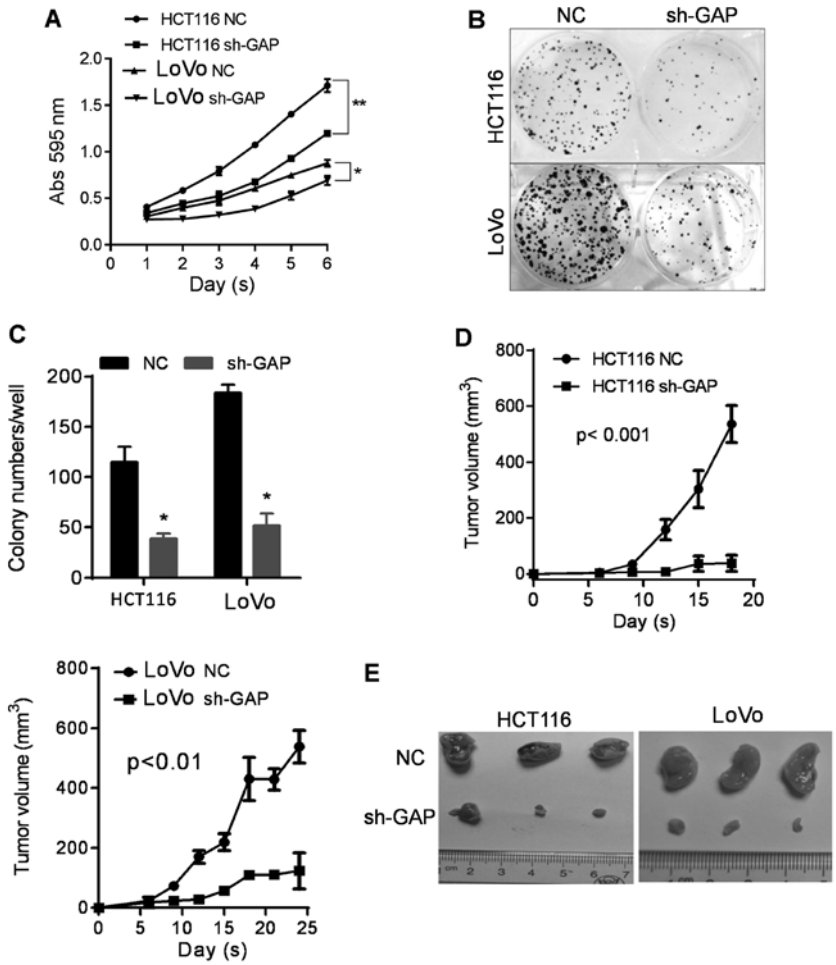

Figure 2. GAPDH knockdown inhibits cancer cell proliferation *in vitro* and tumor growth *in vivo*. (A) Cellular proliferation in sh-GAP and NC cells in both HCT116 and LoVo cell pairs were measured using MTT assay. (B and C) Colony formation in sh-GAP and NC cells of both HCT116 and LoVo cell lines. Cells were seeded in 6-well plates (500 cells/well) for two weeks, and cell colonies of >50 cells were counted and photographed. (D and E) Comparison of tumor growth after sh-GAP and NC cells (both HCT116 and LoVo cell pairs) were subcutaneously innoculated in nude mice. Tumor volume was determined as described in Materials amd methods. At the end of week 3, the animals were sacrificed and the tumors were isolated for comparison (E).

were added sequentially. After the incubation and washing, the tissue slides were stained with the DAB substrate kit, and then stained with hematoxylin.

Statistical analysis. Statistical analysis was performed using the GraphPad Prism software package (v.4.02; GraphPad Software, Inc., La Jolla, CA, USA). The Student's t-test was used to evaluate the statistical significance of the two mean values between two groups. A $P<0.05$ was considered statistically significant.

Results

Suppression of GAPDH by shRNA and its effect on glucose metabolism. To investigate the impact of GAPDH on cancer cell behavior, we first constructed GAPDH knockdown cell lines by stable transfection of HCT116 and LoVo cells with lentivirus vectors containing either shRNA against GAPDH (sh-GAP) or scramble shRNA as a negative control (NC). Stable transfection with sh-GAP significantly reduced the expression of GAPDH in both HCT116 and LoVo cells, as revealed by RT-PCR and western blot analysis (Fig. 1A and B). GAPDH knockdown by shRNA consistently reduced GAPDH activity in both HCT116 and LoVo cells (Fig. 1C). As GAPDH is an important glycolytic enzyme (20), we evaluated glycolytic activity after silencing of GAPDH expression by shRNA, and showed that the sh-GAP cells consumed less glucose and produced less lactate than the NC cells in both HCT116 and LoVo cell pairs (Fig. 1D). These metabolic changes were futher confirmed using a Seahorse XF analyzer. As shown in Fig. 1E, the basal glycolytic activity (basal extracellular acidification rate, ECAR) was lower in HCT116 sh-GAP cells than in HCT116-NC cells, and there was significantly less increase in ECAR in HCT116 sh-GAP cells than in HCT116-NC cells after glucose was injected to the culture medium, indicating that GAPDH knockdown substantially impaired glycolytic capacity. Furthermore, we examined the maximum glycolytic capacity in these two cell lines by using oligomycin to inhibit oxidative phosphorylation. Our results showed that the maximum glycolytic capacity decreased substantially after GAPDH silencing, and that glycolytic reserve was also significantly reduced after GAPDH knockdown in HCT116 cells (Fig. 1E-G). Oxygen consumption rate (OCR) also decreased in HCT116 sh-GAP cells compared with HCT116-NC cells (data not shown). Notably, unlike the control cells that showed an increase in OCR when exogenous glucose was added,

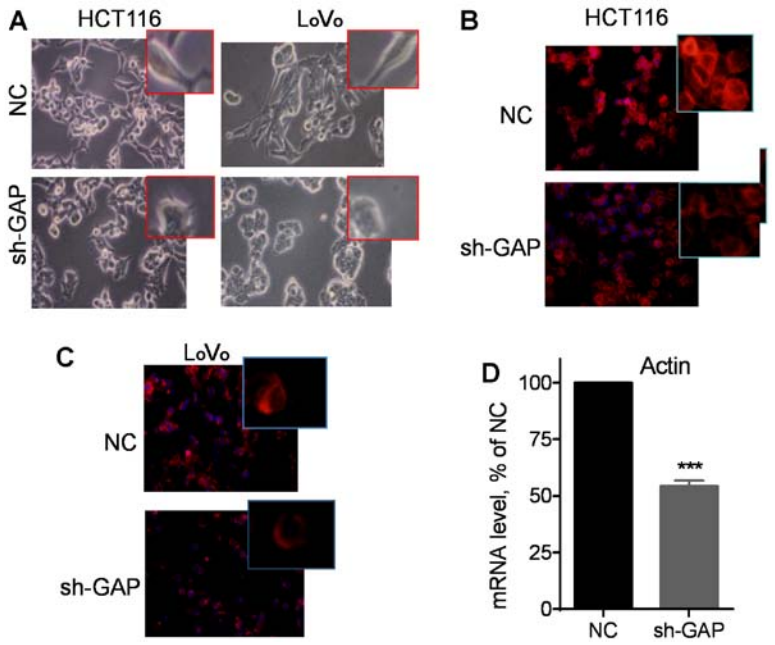

Figure 3. Changes in cell morphology and expression of actin after silencing of GAPDH. (A) Morphology of HCT116 and LoVo cells after stable knockdown of GAPDH expression by lentiviral-shRNA (sh-GAP). The viral vector containing scrambled shRNA was used as negative control (NC). (B) Fluorescent staining of F-actin by phalloidine in HCT116 cells infected with lentiviral vector containing shRNA against GAPDH (sh-GAP) or control shRNA (NC). (C) Fluorescent staining of F-actin by phalloidine in LoVo cells infected with lentiviral vector containing shRNA against GAPDH (sh-GAP) or control shRNA (NC). (D) Expression of actin mRNA in HCT116 cells measured by qRT-PCR. Data are shown as mean ± SD from three separate experiments, $^{***}P<0.001$.

injection of glucose into sh-GAP cells did not increase OCR, suggesting that silencing of GAPDH compromised the ability of cells to use glucose as a substrate for oxidative metabolism in the mitochondria.

Effect of GAPDH on cancer cell proliferation and migration/invasion. Uncontrolled proliferation is a characteristic behavior of cancer cells. MTT and colony formation assays were performed to test the effect of GAPDH silencing on cell proliferation in HCT116 and LoVo cells. As shown in Fig. 2A, cell proliferation was markedly retarded in sh-GAP cells compared to the NC cells in both HCT116 and LoVo cell pairs. Furthermore, GAPDH silencing markedly reduced colony formation ability in both HCT116 and LoVo cell lines, as evidenced by the small size and low number of colonies in the sh-GAP cells compared to NC cells (Fig. 2B and C).

As GAPDH depletion inhibits cell proliferation and colony formation *in vitro*, we further evaluated the impact of GAPDH on tumor formation *in vivo*. HCT116 sh-GAP and LoVo sh-GAP cells were inoculated subcutaneously into athymic nude mice to initiate tumor formation, and the same numbers of the respective NC cell lines were also inoculated in the same fashion as control groups. Tumor growth was monitored for three weeks. As shown in Fig. 2D, tumor growth was significantly retarded in sh-GAP group compared to the NC group. By the end of week 3, the animals were sacrificed and the tumors were isolated for comparison (Fig. 2E). The data confirmed that suppression of GAPDH expression significantly inhibited tumor growth *in vivo*.

Notably, microscopic examination revealed that silencing of GAPDH expression led to apparent changes in cell morphology from the original spindle-like mesenchymal shape to a more polygonal epithelial appearance (Fig. 3A). Fluorescent staining of F-actin using phalloidin revealed that suppression of GAPDH substantially reduced the amount of F-actin in the cytoskeleton filaments, as evidenced by a significant decrease in fluorescent intensity in HCT116 sh-GAP cells (Fig. 3B) and LoVo sh-GAP cells (Fig. 3C). Consistently, quantitative analysis of gene expression by qRT-PCR using a pair of primers for both β-actin and γ-actin showed a significant reduction in actin mRNA expression after silencing of GAPDH (Fig. 3D). These data together suggest that GAPDH might play an important role in the regulation of actin expression and thus, affecting cell motility.

We then used a 'wound healing' assay to evaluate the impact of GAPDH on cell migration. As shown in Fig. 4A, the control HCT116 and LoVo cells migrated and covered ~60-70% scratched area after 48 h, wherea sh-GAP cells only filled approximately 10-30% of the scratched area during the same period. Theses results indicate that GAPDH depletion substantially repressed cell migration. Similar phenomenon was observed in HT29 cells, which expressed much lower GAPDH and migrated significantly slower than HCT116 cells with higher GAPDH expression (Fig. 4B). Furthermore, Transwell and Matrigel invasion assays were performed to compare the migration and the invasion in the NC and sh-GAP cells. As shown in Fig. 4C and D, GAPDH knockdown significantly inhibited cell migration and invasion in both HCT116 and LoVo cells. Consistently, HT29 with low expression of GAPDH also exhibited reduction in invasive capacity compared to HCT116 with high GAPDH expression (Fig. 4E).

Attenuation of EMT and downregulation of SNAIL by silencing of GAPDH. Previous studies suggest that EMT is essential for migration and invasion regulated by SNAIL, which suppresses

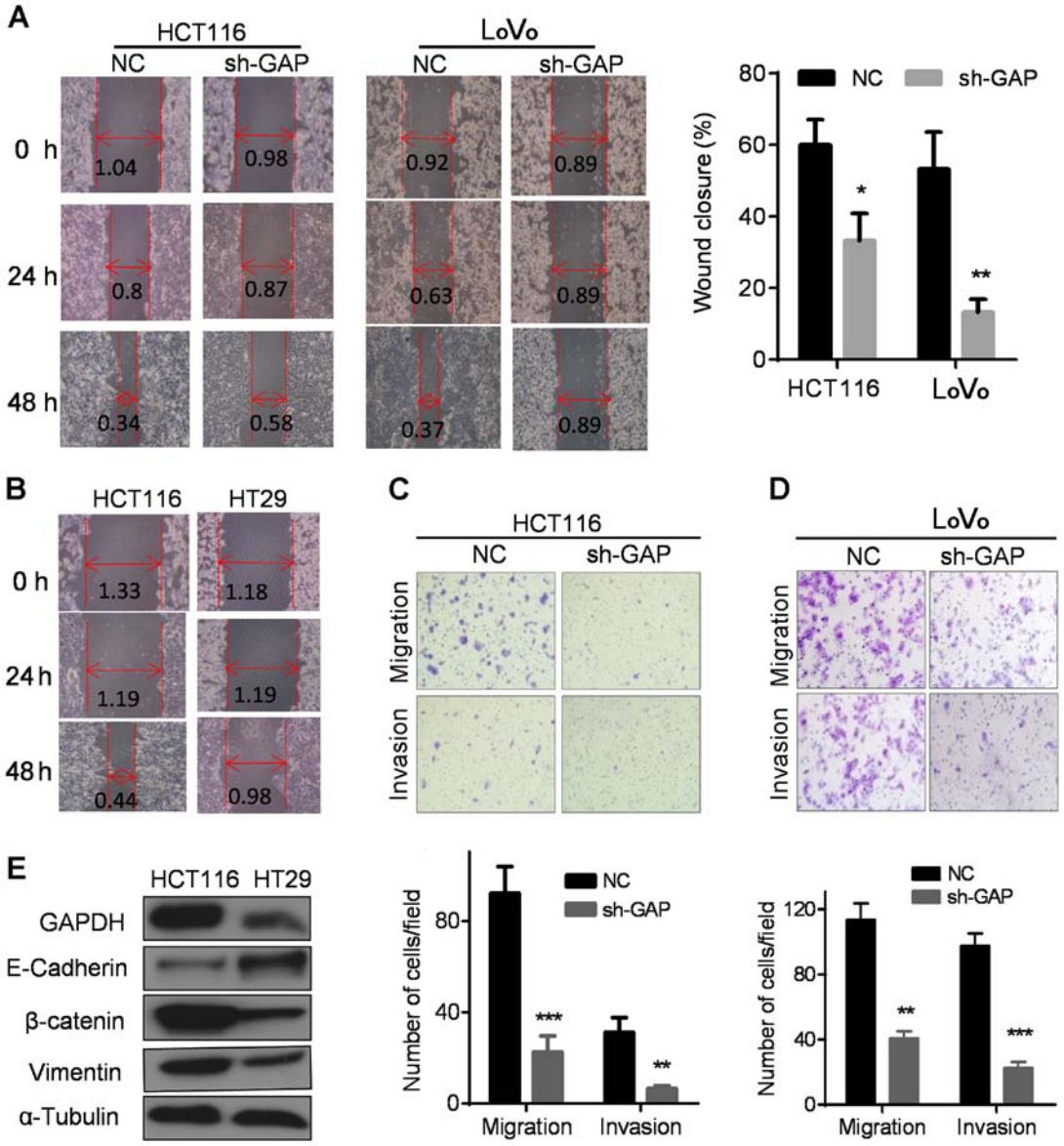

Figure 4. Effect of GAPDH on colorectal cancer cell migration and invasion *in vitro*. (A) Wound healing assay was performed in sh-GAP and NC cells of both HCT116 and LoVo cell pairs. Images were taken at 0, 24 and 48 h after scratching (original magnification, x10). The numbers indicate the average width (in mm) of the scratched areas. The bar graph on the right panel shows the quantitative results of the wound healing, expressed as % of scratched area that was covered by the cells at 48 h. (B) Comparison of cell migration in HCT116 and HT29 cells. The ability of cells to fill the scratched area was evaluated by wound healing assay. (C and D) Representative images of crystal violet-stained sh-GAP and NC cells of HCT116 and LoVo cells that invaded through the Matrigel and migrated through the pores of the membranes were taken 30 h after seeding. The cells that passed the membrane pores were counted in three representative high power fields per Transwell insert. (E) Western blot analysis of protein expression of EMT-related molecules in HCT116 and HT29 cells. α-Tubulin was blotted as a loading control. Migration and invasion of HCT116 and HT29 were measured in Transwell systems without or with Matrigel. Images of cells that migrated through the Transwell membranes were taken 30 h after seeding. Data are shown as mean ± SD. n=3, *P<0.05, **P<0.01, ***P<0.001.

the expression of E-cadherin and upregulates the vimentin and β-catenin, leading to enhancement of EMT (21,22). Therefore, we examined the impact of GAPDH knockdown on expression of EMT-related molecules by western blot analysis. As shown in Fig. 5A, silencing of GAPDH resulted in a suppression of SNAIL expression, associated with an upregulation of E-cadherin and a downregulation β-catenin and vimentin in both HCT116 and LoVo cells. Consistently, a high expression of E-cadherin and a low expreesion of β-catenin and vimentin were also observed in HT29 cells, which expressed a lower level of GAPDH compared to HCT116 cells (Fig. 4E). Quantitative analysis of mRNA by qRT-PCR revealed that SNAIL mRNA expression level was significantly decreased when GAPDH was knocked down by shRNA (Fig. 5B), suggesting that the decrease in SNAIL protein in sh-GAP cells might likely be due to a reduction at the transcriptional level. Since GAPDH protein has been observed to translocate to the nucleus and affect gene expression (16), we speculated that GAPDH might regulate SNAIL transcription by interacting with its promoter. To test this possibility, chromatin immunoprecipitation (ChIP) assay was performed using an antibody against GAPDH to pull down the DNA fragments associated with GAPDH, followed by PCR using a pair of primers specific for *SNAIL* minimal promoter region (nt positions -78 to +59). Non-specific IgG was used as a control for the pulldown. As shown in Fig. 5C and D, pulldown of GAPDH resulted in a

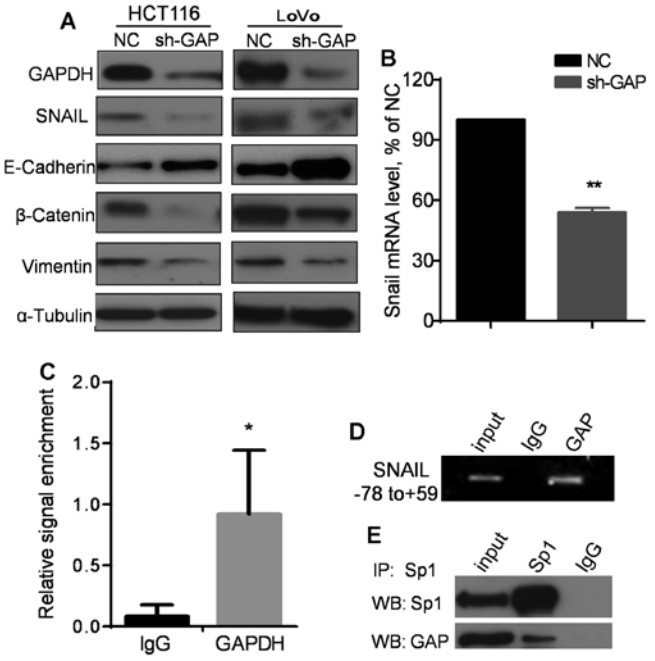

Figure 5. GAPDH knockdown inhibits epithelial-mesenchymal transition (EMT) by suppressing SNAIL expression. (A) Western blot analyis was used to detect the expression of EMT makers in sh-GAP and NC cells of both HCT116 and LoVo cell lines. α-Tubulin was blotted as protein loading control. (B) Expression of SNAIL mRNA in HCT116 sh-GAP cells and HCT116-NC cells, measured by qRT-PCR. (C) Chromatin immunoprecipitation (ChIP)-qPCR was performed in HCT116-NC cells. Sheared DNA was incubated with 1.5 μg anti-GAPDH antibody or control IgG overnight at 4˚C, primers for SNAIL from nt-78 to nt+59 was used to detect possible enrichment of SNAIL signal by qRT-PCR. Normal rabbit IgG served as negative controls. (D) Endpoint PCR was performed to analyze the ChIP-qPCR products. Unsheared DNA was used as a positive control (input). (E) Co-immunoprecipitation (CO-IP) assay was performed with anti-Sp1 antibodies or control IgG in HCT116-NC cells. Immunoprecipitants were subjected to western blot analysis using antibody against Sp1 or GAPDH. Whole cell lysates were used as the positive control (input), while non-specific rabbit IgG was used as negative control (IgG) for IP. Data are shown as mean ± SD (n=3), *P<0.05, **P<0.01.

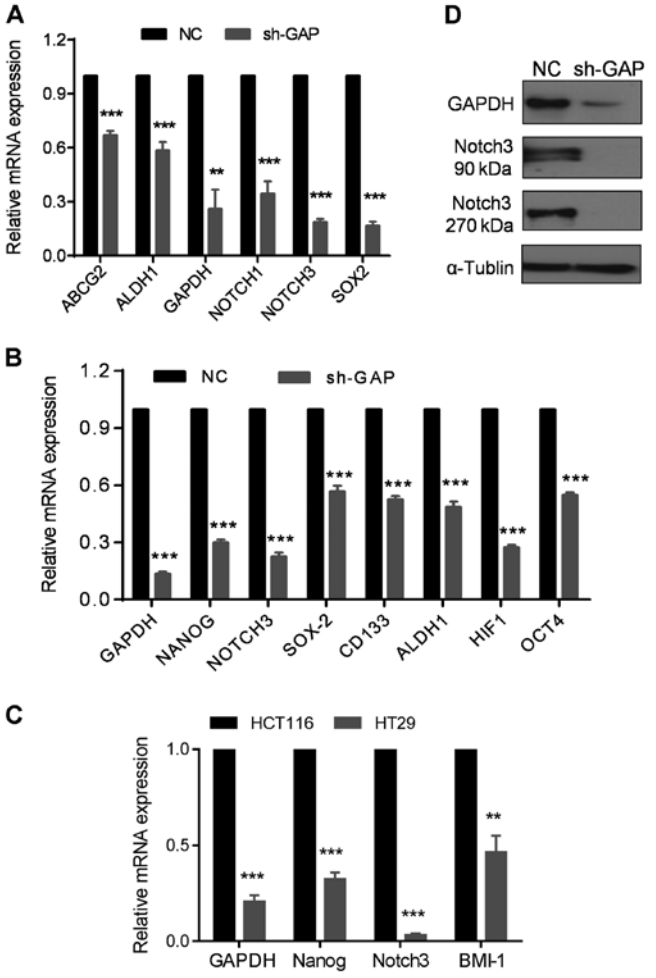

Figure 6. GAPDH knockdown repressed the expression of stem-like cell-related molecules. (A and B) Comparison of mRNA levels of stem-like cell-related molecules in HCT116 sh-GAP and HCT116-NC cells (A) and in LoVo cells (B). Expression of mRNA was detected by RT-PCR. Graph shows mean ± SD; **P<0.01; ***P<0.001. (C) Measurement of mRNA levels of GAPDH, Nanog, Notch3 and BMI1 by qRT-PCR. Data are shown as mean ± SD. n=3, **P<0.01, ***P<0.001. (D) Comparison of NOTCH3 protein expression in LoVo sh-GAP and LoVo-NC cells by western blotting. α-Tubulin was also blotted as the loading control.

sinificant enrichment of PCR signal for the *SNAIL* minimal promoter. Since it is known that the transcriptional factor Sp1 directly binds to *SNAIL* minimal promoter (-78/+59) and enhance its expression to promote EMT (23), we tested if Sp1 and GAPDH were physically associated with each other by co-immunoprecipitation assay. As shown in Fig. 5E, Sp1 and GAPDH were co-precipitated by the Sp1 antibody, while immunoprecipitation using control IgG yield negative signal, suggesting a direct physical interaction between GAPDH and Sp1.

Regulation of stem-like cell markers by GAPDH. Since EMT is closely associated with stem-like cell properties, we examined the expression of stem-like cell markers in sh-GAP and NC cells. Strikingly, most of the stem cell-related markers including *ABCG2*, *ALDH1*, *SOX2*, *OCT4*, *CD133*, *NOTCH1*, *NOTCH3* and *NANOG* were substantially decreased after GAPDH silencing, as shown by qRT-PCR assay (Fig. 6A and B). The expressions of *NOTCH3*, *NANOG* and *BMI1* were also reduced in HT29 with lower expression of GAPDH compared to HCT116 (Fig. 6C). Consistently, expression of NOTCH3 protein was abolished when GAPDH expression was suppressed by shRNA, as evidenced by the disappearance of both the 90-kDa extracellular domain of NOTCH3 and the 270-kDa NOTCH3 protein (Fig. 6D). These results indicate that silencing of GAPDH expression could significantly down-regulate the expression of stem cell-related molecules.

Impact of GAPDH on tumor invasion and lung metastasis in vivo. Based on the observations that GAPDH depletion reduced cell migration and invasion *in vitro*, we conducted animal experiments to evaluate the impact of GAPDH on tumor invation and metastasis *in vivo*. As shown in Fig. 7A and B, two control cancer cell lines (HCT116-NC and LoVo-NC) with high GAPDH expression exhibited invasive phenotype in the subcutaneous tumor xenografts with noticeable clusters of tumor cells invading into the adjacent tissues, while shRNA silencing of GAPDH expression in HCT116 and LoVo cells (sh-GAP) suppressed the invasive behavior.

We then compared the abilities of the HCT116 sh-GAP cells and HCT116-NC cells to form distant metastasis in

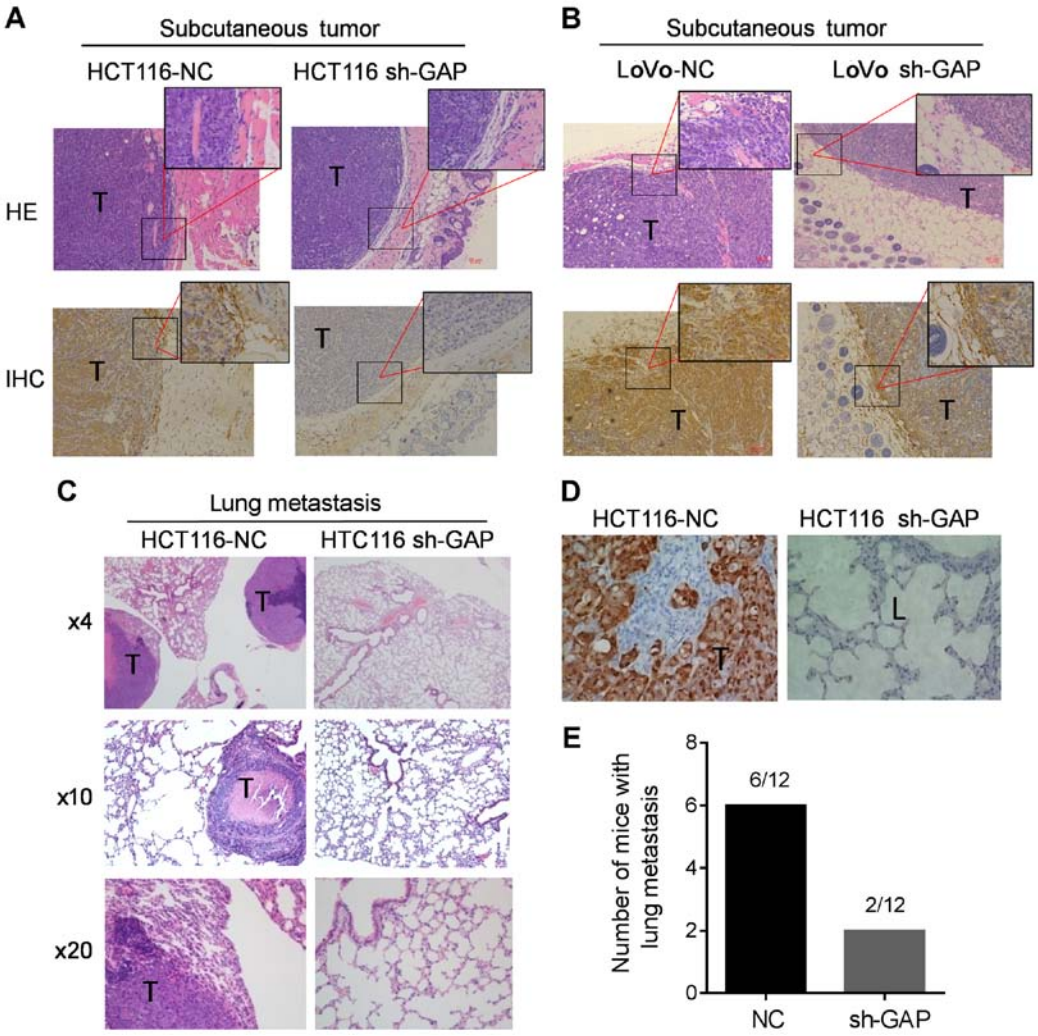

Figure 7. Silencing of GAPDH inhibited cancer cell invasion and lung metastasis *in vivo*. (A and B) Nude mice were subcutaneously inoculated with HCT116 sh-GAP, HCT116-NC, LoVo sh-GAP and LoVo-NC cells. Tumors tissues were subjected to H&E staining (top panels) or immunostaining with anti-GAPDH antibody (bottom panels); T, indicates tumor tissue. (C) HCT116 sh-GAP or HCT116-NC cells were injected into BALB/C nude mice (12 mice/group) through tail veins. After one and a half months, the mice were sacrificed and the lungs were isolated for examination of metastasis. Paraffin-embedded slides were stained with H&E. (D) Immunohistochemistry staining of GAPDH of the lung tissues from mice injected (tail vein) with HCT116 sh-GAP or HCT116-NC cells. T, tumor tissue; L, lung tissue. (E) Number of mice with lung metastasis 6-7 weeks after tail-vein injection of HCT116 sh-GAP cells or HCT116-NC cells. The numbers 2/12 and 6/12 indicate the numbers of mice with lung metastasis per group of 12 mice.

mouse models. The same number of sh-GAP and NC cells was injected into the tail veins of 6-week old nude mice. After 45 days, the mice were sacrificed and lung metastasis were examined (Fig. 7C), and the expression of GAPDH in the tumor and adjacent tissue was revealed by immunohistochemistry staining (Fig. 7D). The results showed that HCT116-NC cells with high GAPDH expression developed large tumors in the lung, whereas the ability of sh-GAP cells to form tumors in the lung was significantly reduced (Fig. 7E). These data further confirm that GAPDH plays an important role in colon cancer invasion and metastasis *in vivo*.

Discussion

Under physiological conditions, normal cells rely on the more energy-efficient oxidative phosphorylation to generate ATP. In contrast, many cancer cells actively use the glycolytic pathway for ATP generation even in the presence of adequate oxygen, a phenomenon known as the Warburg effect (24). GAPDH is an important glycolytic enzyme and its high expression in cancer cells seems to be associated with aggressive malignant behavior of the cancer cells and is also associated with poor prognosis of lung cancer patients (25-27). Our previous study showed that high GAPDH expression was associated with cancer metastasis (18), but the underlying mechanism remains unclear. The main goals of the study were to use biochemical and genetic strategies to establish defined cell models to evaluate the impact of GAPDH on cancer cell behavior *in vitro* and *in vivo* relevant to metastasis, and to investigate the possible regulatory mechanisms.

Cancer metastasis is a complex process involving multiple steps from detachment of cancer cells from the original/primary tumor to establishment of new cancer colonies at the distant tissue sites. This process requires the concerted action of various proteins that affect cell adhesion, migration, invasion and survival at the target tissues (28). EMT is associated with certain key steps in this process involving cell migration and invasion, and is also considered as a stem-like cell phenotype

(19,29). In the present study, we demonstrated that silencing of GAPDH significantly abrogated the EMT phenotype of colon cancer cells in both HCT116 and LoVo cells lines, and inhibited cell migration and invasion *in vitro* and tumor metastasis *in vivo*. These data strongly suggest that GAPDH may play an important role in promoting metastasis, at least in colon cancer. At the molecular level, GAPDH seems to physically intereact with Sp1, a key transcriptional factor known to bind to the promoter of SNAIL and enhance its expression (23,30). It seems possible that GAPDH forms a protein complex with Sp1 and enhance to expression of SNAIL, which is a transcriptional inducer of EMT (31). Indeed, we showed that shRNA silencing of GAPDH expression led to a significant decrease of SNAIL expression in both HCT116 and LoVo cells, accompanied by an upregulation of E-cadherin and a downregulation of β-catenin and vimentin (Fig. 5A). Consistent with these observations, there was a significant decrease in F-actin formation and an apparent reversion of essenchymal cell morphology to epithelial appearance after knockdown of GAPDH expression. These data together support a possibility that GAPDH may promote EMT and cancer metastasis by enhancing Sp1-mediated expression of SNAIL.

GAPDH is a molecule with enzymatic activity in glycolysis in the cytoplasma and non-enzymatic functions in the nucleus (13-16,20). Although we showed that silencing of GAPDH significantly attenuate glycolysis and other relevant metabolism, it is unclear if such metabolic changes play any significant role in affecting metastasis. One possibility is that GAPDH might affect cell mobility and metastasis indirectly by affecting energy (ATP) generation through its metabolic function in glycolysis. We indeed observed that a knockdown of GAPDH expression led to significant decrease in glycolysis and an inhibition of cell migration and invasion. However, we could not exclude the possibility that the reduced glycolysis and decreased cell migration were two parallel events without causal relationship. Another possibility is that GAPDH affects cell migration and cancer metastasis mainly through its non-metabolic function. A previous study showed that GAPDH would translocate to nucleus when cells encountered certain stress conditions such as oxidative stress in cancer cells. Oxidative stress-induced S-nitrosylation of GAPDH could promote translocation of GAPDH to nucleus (15), where it could intereact with Sp1 under oxidative stress conditions, and activate *SNAIL* transcription. Thus, it is possible that GAPDH may promote EMT and metastasis through its non-enzymatic function in the nucleus. Further research is required to clearly define the relative contribution of metabolic and transcriptional function of GAPDH in promoting cancer metastasis. Generation of GAPDH mutants with change in either enzyme activity or transcriptional activity would provide important tools for such study.

It is interesting to note that silencing of GAPDH expression led to downregulation of SNAIL and decreased expression of stem cell markers including ABCG2, ALDH1, SOX2, OCT4, CD133, NOTCH1, NOTCH3, NANOG and BMI1. Although the exact relationship between EMT and cancer stem cells still remains unclear and somewhat controversial, emerging evidence suggest a close association between EMT and cancer stem cell phenotype. For instance, a recent study suggests that SNAIL could promote EMT and increase the expression of stem cell markers in colon cancer cells leading to an enhancement of cancer cell invasion and metastasis (31). Another study showed that silencing stem cell regulator SOX2 could induced a reversion of EMT known as mesenchymal-epithelial transition (32). Consistent with these observations, our findings that a knockdown of GAPDH resulted in a downregulation of SNAIL and stem-related molecules and led to morphological changes of colon cancer cells from the spindle-like mesenchymal shape to a polygonal epithelial appearance support the notion that EMT and stemness of cancer cells are linked.

In summary, the present study suggests that GAPDH may play an important role in promoting cancer metastasis through upregulation of Sp1-mediated expression of SNAIL, leading to epithelial-mesenchymal transition and enhancement of cellular migration and invasion. As such, it may be possible to prevent or inhibit colon cancer metastasis by silencing GAPDH through genetic manipulation or chemical inhibtion. Future studies are needed to test GAPDH and its downstream molecules as therapeutic targets in metastatic colon cancer.

Acknowledgements

The present study was supported in part by grants from the National Natural Science Foundation of China (nos. 81430060 and 81502573), the Guangzhou Innovation Research Program (no. LCY201317), the Guangzhou Medicare Collaborative Innovation Program (no. 201508020250) and the 2014A030310421 from the Natural Science Foundation of Guangdong Province.

References

1. Martins SF, Garcia EA, Luz MA, Pardal F, Rodrigues M and Filho AL: Clinicopathological correlation and prognostic significance of VEGF-A, VEGF-C, VEGFR-2 and VEGFR-3 expression in colorectal cancer. Cancer Genomics Proteomics 10: 55-67, 2013.
2. Weitz J, Koch M, Debus J, Höhler T, Galle PR and Büchler MW: Colorectal cancer. Lancet 365: 153-165, 2005.
3. Des Guetz G, Uzzan B, Nicolas P, Cucherat M, Morere JF, Benamouzig R, Breau JL and Perret GY: Microvessel density and VEGF expression are prognostic factors in colorectal cancer. Meta-analysis of the literature. Br J Cancer 94: 1823-1832, 2006.
4. Martins SF, Reis RM, Rodrigues AM, Baltazar F and Filho AL: Role of endoglin and VEGF family expression in colorectal cancer prognosis and anti-angiogenic therapies. World J Clin Oncol 2: 272-280, 2011.
5. Barderas R, Mendes M, Torres S, Bartolomé RA, López-Lucendo M, Villar-Vázquez R, Peláez-García A, Fuente E, Bonilla F and Casal JI: In-depth characterization of the secretome of colorectal cancer metastatic cells identifies key proteins in cell adhesion, migration, and invasion. Mol Cell Proteomics 12: 1602-1620, 2013.
6. Arlt F and Stein U: Colon cancer metastasis: MACC1 and Met as metastatic pacemakers. Int J Biochem Cell Biol 41: 2356-2359, 2009.
7. O'Connell JB, Maggard MA and Ko CY: Colon cancer survival rates with the new American Joint Committee on Cancer sixth edition staging. J Natl Cancer Inst 96: 1420-1425, 2004.
8. Murata K and Moriyama M: Isoleucine, an essential amino acid, prevents liver metastases of colon cancer by antiangiogenesis. Cancer Res 67: 3263-3268, 2007.
9. Iqbal S and Lenz HJ: Angiogenesis inhibitors in the treatment of colorectal cancer. Semin Oncol 31 (Suppl 17): 10-16, 2004.
10. El Zouhairi M, Charabaty A and Pishvaian MJ: Molecularly targeted therapy for metastatic colon cancer: Proven treatments and promising new agents. Gastrointest Cancer Res 4: 15-21, 2011.

11. Mori R, Wang Q, Danenberg KD, Pinski JK and Danenberg PV: Both beta-actin and GAPDH are useful reference genes for normalization of quantitative RT-PCR in human FFPE tissue samples of prostate cancer. Prostate 68: 1555-1560, 2008.
12. Murthi P, Fitzpatrick E, Borg AJ, Donath S, Brennecke SP and Kalionis B: GAPDH, 18S rRNA and YWHAZ are suitable endogenous reference genes for relative gene expression studies in placental tissues from human idiopathic fetal growth restriction. Placenta 29: 798-801, 2008.
13. Harada N, Yasunaga R, Higashimura Y, Yamaji R, Fujimoto K, Moss J, Inui H and Nakano Y: Glyceraldehyde-3-phosphate dehydrogenase enhances transcriptional activity of androgen receptor in prostate cancer cells. J Biol Chem 282: 22651-22661, 2007.
14. Tisdale EJ: Glyceraldehyde-3-phosphate dehydrogenase is required for vesicular transport in the early secretory pathway. J Biol Chem 276: 2480-2486, 2001.
15. Sirover MA: On the functional diversity of glyceraldehyde-3-phosphate dehydrogenase: Biochemical mechanisms and regulatory control. Biochim Biophys Acta 1810: 741-751, 2011.
16. Zheng L, Roeder RG and Luo Y: S phase activation of the histone H2B promoter by OCA-S, a coactivator complex that contains GAPDH as a key component. Cell 114: 255-266, 2003.
17. Epner DE, Partin AW, Schalken JA, Isaacs JT and Coffey DS: Association of glyceraldehyde-3-phosphate dehydrogenase expression with cell motility and metastatic potential of rat prostatic adenocarcinoma. Cancer Res 53: 1995-1997, 1993.
18. Tang Z, Yuan S, Hu Y, Zhang H, Wu W, Zeng Z, Yang J, Yun J, Xu R and Huang P: Over-expression of GAPDH in human colorectal carcinoma as a preferred target of 3-bromopyruvate propyl ester. J Bioenerg Biomembr 44: 117-125, 2012.
19. Thiery JP and Sleeman JP: Complex networks orchestrate epithelial-mesenchymal transitions. Nat Rev Mol Cell Biol 7: 131-142, 2006.
20. Sirover MA: New nuclear functions of the glycolytic protein, glyceraldehyde-3-phosphate dehydrogenase, in mammalian cells. J Cell Biochem 95: 45-52, 2005.
21. Zhou BP, Deng J, Xia W, Xu J, Li YM, Gunduz M and Hung MC: Dual regulation of Snail by GSK-3beta-mediated phosphorylation in control of epithelial-mesenchymal transition. Nat Cell Biol 6: 931-940, 2004.
22. Peña C, García JM, Silva J, García V, Rodríguez R, Alonso I, Millán I, Salas C, de Herreros AG, Muñoz A, *et al*: E-cadherin and vitamin D receptor regulation by SNAIL and ZEB1 in colon cancer: Clinicopathological correlations. Hum Mol Genet 14: 3361-3370, 2005.
23. Barberà MJ, Puig I, Domínguez D, Julien-Grille S, Guaita-Esteruelas S, Peiró S, Baulida J, Francí C, Dedhar S, Larue L, *et al*: Regulation of Snail transcription during epithelial to mesenchymal transition of tumor cells. Oncogene 23: 7345-7354, 2004.
24. Warburg O: On the origin of cancer cells. Science 123: 309-314, 1956.
25. Tokunaga K, Nakamura Y, Sakata K, Fujimori K, Ohkubo M, Sawada K and Sakiyama S: Enhanced expression of a glyceraldehyde-3-phosphate dehydrogenase gene in human lung cancers. Cancer Res 47: 5616-5619, 1987.
26. Révillion F, Pawlowski V, Hornez L and Peyrat JP: Glyceraldehyde-3-phosphate dehydrogenase gene expression in human breast cancer. Eur J Cancer 36: 1038-1042, 2000.
27. Puzone R, Savarino G, Salvi S, Dal Bello MG, Barletta G, Genova C, Rijavec E, Sini C, Esposito AI, Ratto GB, *et al*: Glyceraldehyde-3-phosphate dehydrogenase gene over expression correlates with poor prognosis in non small cell lung cancer patients. Mol Cancer 12: 97, 2013.
28. Nguyen DX and Massagué J: Genetic determinants of cancer metastasis. Nat Rev Genet 8: 341-352, 2007.
29. Beerling E, Seinstra D, de Wit E, Kester L, van der Velden D, Maynard C, Schäfer R, van Diest P, Voest E, van Oudenaarden A, *et al*: Plasticity between epithelial and mesenchymal states unlinks EMT from metastasis-enhancing stem cell capacity. Cell Rep 14: 2281-2288, 2016.
30. Higashimura Y, Nakajima Y, Yamaji R, Harada N, Shibasaki F, Nakano Y and Inui H: Up-regulation of glyceraldehyde-3-phosphate dehydrogenase gene expression by HIF-1 activity depending on Sp1 in hypoxic breast cancer cells. Arch Biochem Biophys 509: 1-8, 2011.
31. Fan F, Samuel S, Evans KW, Lu J, Xia L, Zhou Y, Sceusi E, Tozzi F, Ye XC, Mani SA, *et al*: Overexpression of snail induces epithelial-mesenchymal transition and a cancer stem cell-like phenotype in human colorectal cancer cells. Cancer Med 1: 5-16, 2012.
32. Han X, Fang X, Lou X, Hua D, Ding W, Foltz G, Hood L, Yuan Y and Lin B: Silencing SOX2 induced mesenchymal-epithelial transition and its expression predicts liver and lymph node metastasis of CRC patients. PLoS One 7: e41335, 2012.